

Daniel R. Chavas* and Michael C. Morgan

University of Wisconsin – Madison
Madison, Wisconsin

1. INTRODUCTION

African easterly waves (AEWs) are lower-tropospheric disturbances that travel westward across western Africa and the tropical Atlantic during the Northern Hemisphere summer. These systems are widely believed to originate from both barotropic and baroclinic growth mechanisms within the West African Mid-tropospheric Easterly Jet (Burpee 1972; Rennick 1976; Thorncroft and Hoskins 1994; and references therein). Radiosonde observations from Dakar, Senegal and global meteorological analyses from the ECMWF indicate that these disturbances cross the west African coast approximately every 3-5 days (Burpee 1972; Reed et al. 1988). Spectral analyses of the meridional-wind variance throughout the depth of the troposphere, based on time series at various radiosonde stations across central and western Africa, suggest that the AEW amplitude is strongest near 700 hPa and weakens with height (e.g., Burpee 1972). The meridional width of the vorticity perturbations typically extends across 20° of latitude, while the zonal length scale of these perturbations is of order 1000 km (Reed et al. 1977).

African easterly waves progress through different basic-state flow patterns during their trek across the Atlantic. Work by Shapiro (1977) suggested that mean-flow variations across AEWs act to trigger tropical depression development by transforming their structure from a plane-wave form into an isolated-vortex configuration. Though the details of this evolution were not explained, the physical mechanism by which the structural alteration occurs relies on the mean winds' distortion of the original disturbance in a manner that strengthens the nonlinear advection of eddy vorticity. This nonlinearity then transforms the AEW from a wavelike feature into a vortical circulation.

A study by Mak and Cai (1989) on the barotropic growth of disturbances in zonally inhomogeneous basic flows supports the idea that the mean flow plays a significant role in determining which AEWs become depressions. Their results showed that eddies, when elongated along the axis of contraction of the basic deformation field, optimally extract kinetic energy (KE) from the basic state. This is consistent with the principle of PV superposition, whereby anisotropic vortex structures intensify through favorable deformation by the basic-state flow (Farrell 1989b, Mak and Cai 1989, Dole 1993). In short, for continuous distributions of PV, it may be stated that *any processes which tend to make a*

PV anomaly more isotropic results in an increase in the disturbance kinetic energy. AEWs subject to deformation by the basic-state flow, depending on their orientation relative to the mean contraction axes, can thus intensify.

An observational investigation into the development of easterly-wave type disturbances over the western Pacific region by Sobel and Bretherton (1999) concurs with the notion that barotropic mean-to-eddy conversion mechanisms are important in their transformation into tropical depressions. Sobel and Bretherton concluded that the accumulation of Rossby wave activity associated with easterly-wave propagation over that region, which was shown to lead to significant easterly-wave growth rates, was primarily driven by the convergence of the mean flow. Despite the significance of these contributions to our understanding of the growth of disturbances in particular background states, the ways in which AEWs respond to different basic states, the degree to which deformation by the mean flow contributes to their intensification, and the mean-flow orientations that most effectively promote growth, remain enigmas.

In the presentation to follow, we present the results of a composite evolution of AEWs in an AEW following reference frame relative to the time the AEW was declared a depression. This composite is used to assess the propagation speed and steering of these waves, and also to present evidence suggesting that AEWs are not waves (or "wave-like") but rather exist as lower tropospheric coherent vortices somewhat akin to mid-latitude "short waves" as described by Hakim (2000).

2. DATA and METHODOLOGY

a) Data

The data used in this study are derived from the 6-hourly National Center for Environmental Protection (NCEP) 1.0 x 1.0 latitude-longitude, 50 hPa vertical resolution, final analyses available from the National Center for Atmospheric Research (NCAR) Data Support Services as dataset DS083.2.

b) PV diagnostics

The use of PV and PV inversion has proved helpful in clarifying our understanding of tropical cyclones, and tropical cyclone (TC) steering. PV diagnostics has been used to quantify TC steering. Wu and Emanuel (1995a,b; hereafter WE1 and WE2) analyzed the effects of the ambient flow on the propagation of a TC using piecewise PV inversion. It is widely accepted that TCs can be viewed as coherent, isolated vortices immersed in a background flow, and are thus steered by a flow

*Corresponding author address: Daniel R. Chavas,
1225 W. Dayton Street, Madison, WI 53706; email:
drchavas@wisc.edu

(the “steering flow”) which can be approximated by a balanced or pressure-weighted average of the ambient horizontal winds within a prescribed radial distance from the center of the storm. Chan and Gray [1982, (hereafter CG)] evaluated the efficacy of several different techniques for steering flow measurement that varied by pressure layer, method of integration, radial extent of the flow from the center, and intensities and locations of storms.

While there are a number of examples of PV “doing” applied to TCs, there are relatively few studies that have made use of PV diagnostics to AEW structure or evolution. In this work, we make use of PV and PV inversion diagnostics to describe AEW structure and propagation. As a first step, we choose to study the AEWs in a quasi-geostrophic framework because of its ease of use given its linear inversion operator. This work will utilize quasi-geostrophic potential vorticity (QGPV) is given by:

$$q_p = f_0 + \beta_0 y + \frac{1}{f_0} \nabla^2 \phi' + \frac{\partial}{\partial p} \left(\frac{f_0}{S} \frac{\partial \phi'}{\partial p} \right),$$

where $f_0 + \beta_0 y$ represents the Coriolis parameter, ϕ' is the deviation geopotential from the reference state (taken to be the U.S. Standard Atmosphere), and S is the reference state static stability parameter. The QGPV is inverted using Neumann boundary conditions, wherein the temperature at 1000 hPa and 100 hPa is specified.

b) Compositing Technique

A composite of the QGPV associated with 17 tropical cyclones between 2000 and 2005 that developed from a “strong African Easterly Wave,” as characterized by the National Hurricane Center’s (NHC’s) six-hourly tropical discussions was constructed. For each wave, the corresponding QGPV was calculated at 6-hour time intervals (0000, 0600, 1200, 1800 UTC) from the time of tropical depression declaration (by the NHC) backwards, within a domain from [1N, 35N] latitude and [100W, 1W] longitude as shown in Fig. 1. Subtraction of a time-mean QGPV field (in this case an 8-day time-mean, although the choice is somewhat arbitrary) removes the large-scale QGPV, resulting in a perturbation PV field that is dominated by the AEW (a positive PV “blob”) and any other smaller PV anomalies in the region. Inversion of the anomalous QGPV results in the associated anomalous (negative) geopotential fields. For each wave, the geopotential minimum in the immediate vicinity of the wave was designated as the wave center, aided by approximate wave locations given by archived NOAA tropical prediction center tropical discussions. The composite at each time interval (e.g., for each wave at 0, 6, 12 etc. hours prior to NHC tropical depression declaration) was then created as a wave-average QGPV field in a 31 x 31 degree box centered on each disturbance.

c) “PV surgery”

Piecewise PV inversion is performed to separate the localized AEW PV anomaly from the larger-scale background flow. Inversion of the difference between

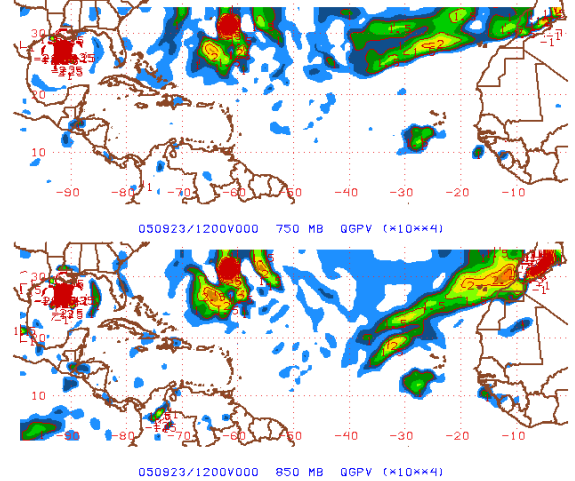


Figure 1. QGPV (fill interval, s^{-1}) at 1200 UTC 23 September 2005 on the 750 hPa and 850 hPa isobaric surfaces. A robust AEW can be seen at approximately 28W 12N.

the total PV field from the AEW PV provides the geopotential (and corresponding geostrophic wind fields) of the ambient flow. The environmental wind field in the vicinity of the composite wave, or the “[TC] advection flow” (WE1), can then be analyzed using a variety of techniques (CG) to determine the speed and direction of wave propagation (Reed *et al.* 1977, hereafter R77), as well as the deformation of the AEW PV structure by the background flow.

3. RESULTS AND DISCUSSION

The 750 hPa and 850 hPa QGPV distributions for 1200 UTC 23 September 2005 are shown in Fig. 1. An AEW was located in the far eastern Atlantic near 12N, 28W. The QGPV associated with this wave is isolated and not part of an undulation of PV contours that would characterize a linear wave. This distribution is not unique – an inspection of these analyses during the 2005 Atlantic hurricane season revealed that most AEW’s are associated with this local PV maxima. Qualitative comparisons between this distribution and Ertel PV for the 2005 Atlantic hurricane season reveal that they are quite similar in structure. Thus, for qualitative purposes at least, the QGPV is a useful tool to track AEWs.

The first step in the wave evolution analysis was the creation of a composite wave evolution. The composite wave was created and examined for a 144-h period prior to tropical depression (TD) declaration. However, several of the 17 waves analyzed either were not within the domain (or were still over Africa) or were too weak during the earlier time periods for inclusion in the compositing. Thus, all 17 waves are included only from 0h-42h prior to TD declaration and 16 waves are included at 48 hours back. For brevity, we restrict our discussion to 30h before genesis (G-30h). The composite wave position at TD declaration was 12.8N, 41.8W.

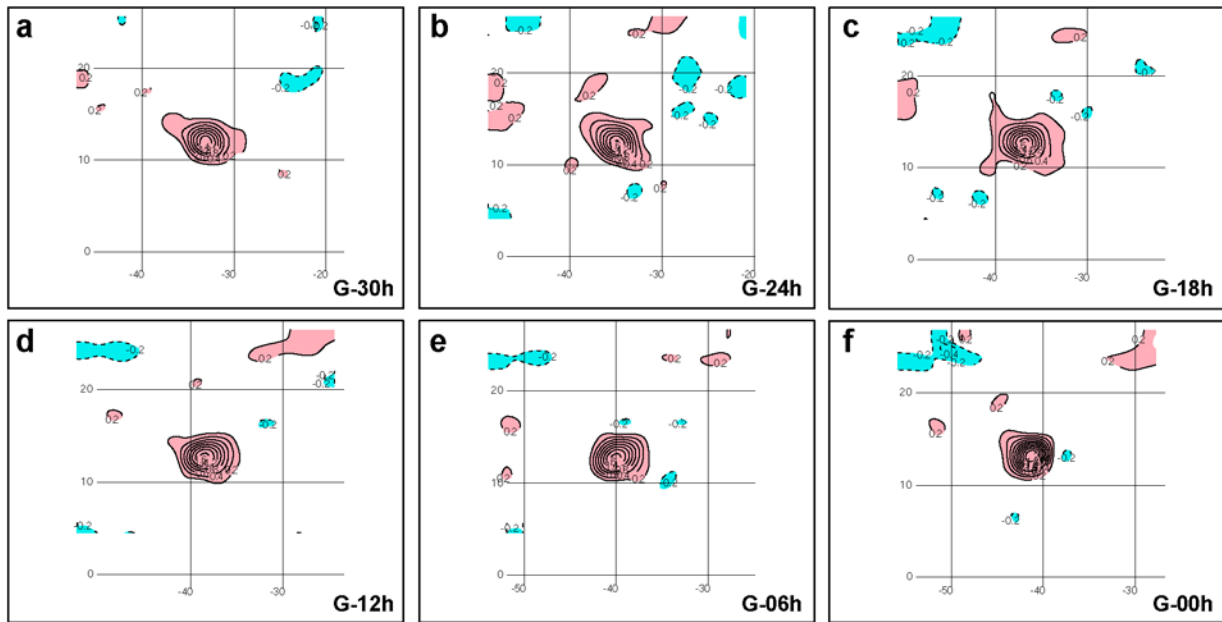


Figure 2. Perturbation QGPV at 850 hPa (interval $.2 \times 10^{-4} \text{s}^{-1}$; positive (negative) values solid (dashed)) for times (a) G-30h, (b) G-24h, (c) G-18h, (d) G-24h, (e) G-06h, and (f) G-00h. Positive (negative) QGPV values are shaded red (blue) above (below) 0.2PVU (-0.2PVU).

a) Propagation speed

The propagation speed of AEWs is calculated by an estimate of the magnitude of the vector speed of the wave composite between each paired time interval (e.g. 0h-6h back from TD) from 0h-42h back, during which all 17 waves are included. The speeds for each time interval are then averaged. The resulting AEW average velocity vector is approximately:

$$c_{AEW} = (-8.5, 1) \text{ms}^{-1} = (-6.8^\circ, 0.8^\circ) \text{day}^{-1},$$

with a wave speed, $|c_{AEW}| = 8.54 \text{ m/s} = 6.85 \text{ deg/day}$.

These calculations have errors due to the relatively high degree of inaccuracy of measurements rounded to the nearest .1 degree (typical meridional speed was ± 0.1 or $\pm 0.2 \text{ deg/day}$). However, these numbers agree closely with that of R77, whose compositing of 8 AEWs from 23 Aug-19 Sep 1974 resulted in an average propagation speed of approximately 8 m/s ($6-7 \text{ deg longitude/day}$), with an assumed meridional speed of zero.

a) PV structure and evolution

Figure 2 shows the composite 850hPa QGPV perturbation field ($q_p' = q_p - q_{\text{mean}}$) at 6h intervals from 30h preceding tropical cyclogenesis declaration (declaration that a depression had formed; G-30h) to the time of genesis (G-00h). These figures further support out contention that AEWs perhaps should not be viewed "waves," but as coherent that are isolated from the environmental flow.

One specific feature that seems common at the 850 hPa level is a northwest-southeast tilt to the wave PV, especially from G-30h to G-18h (Figs. 2a, b, and c). This structure may be the result of the influence of the small negative PV anomalies to the northeast of the composite wave at these times. These anomalies

would induce an anticyclonic circulation that could perhaps result in the observed NW-SE wave deformation. Further examination reveals that these small negative anomalies appear less prevalent directly northeast of the wave anomaly at 0h-18h back (Figs. 2. d-e), and are virtually non-existent at TD declaration (Fig. 2f) except for immediately to the east of the wave. The significance of these smaller-scale anomalies is not known at this time and further quantitative analysis is required for any concrete conclusions to be made regarding their effects and persistence.

The wave at G-00h (Fig. 2f) appears to be far more isotropic than at earlier time, which provides preliminary support for the hypothesis of the initiation of tropical cyclogenesis due to PV anomaly compaction. Furthermore, it is clear that the wave intensity increases with time (as measured by the QGPV): the 850 hPa maximum PV contour is about $1.4 \times 10^{-4} \text{s}^{-1}$ at G-30h then increases to $2 \times 10^{-4} \text{s}^{-1}$ at G-00h.

Figure 3 depicts the vertical-zonal cross section evolution of the composite perturbation QGPV at the wave central latitude for each time from G-30h to G-00h. This discrete time-series shows the development of a "PV tower" from an initially relatively shallow PV anomaly over the 30h intervals leading to TC declaration. At G-30h, the wave is characterized by a westward tilted with height PV anomaly maximized in the lower troposphere, and a weaker, upper tropospheric QGPV anomaly at 200 hPa. The AEW PV extends upward to about 300 hPa. By G-00h the PV tower appears to reach to the top of the troposphere, and is clearly far more isotropic than the prior composite times. At TD declaration, the tower is nearly perfectly vertical, with the maximum altitude for each PV contour

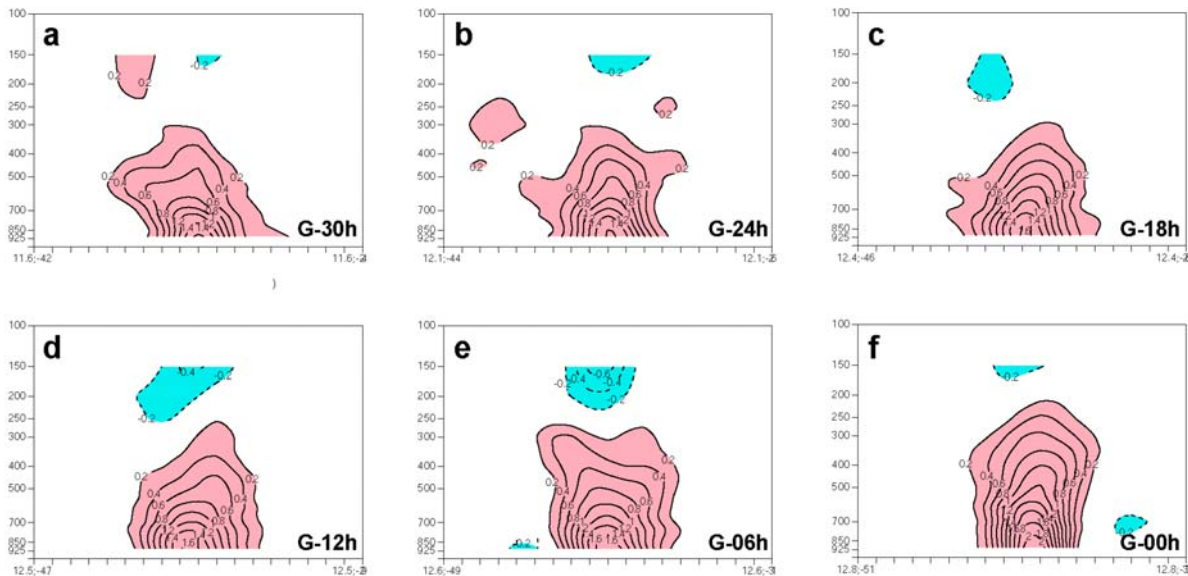


Figure 3. Zonal-height cross sections of perturbation QGPV (interval $.2 \times 10^{-4} \text{s}^{-1}$; positive (negative) values solid (dashed)) for times (a) G-30h, (b) G-24h, (c) G-18h, (d) G-12h, (e) G-06h, and (f) G-00h. Positive (negative) values are shaded red (blue) for QGPV above (below) 0.2PVU (-0.2PVU).

nearly aligned.² Overall, the trend towards a more upright, taller, and more tightly packed PV tower when approaching TD declaration is evident, which, following PV superposition theory, qualitatively supports the hypothesis of kinetic energy extraction from PV superposition leading to the initiation of tropical cyclogenesis.

Figures 4 a-f depict perturbation geopotential fields attributed to the perturbation QGPV (shown in Fig. 3) and the boundary thermal perturbations from G-30h to G-00h for the same domains as in Fig. 3. Over the 40h leading up to tropical cyclogenesis, the lower tropospheric geopotential associated with the wave slowly decreases, while aloft an increase in geopotential is observed in the composite. This increase in upper tropospheric geopotential is consistent with the emergence at 18h prior to TD declaration of an upper-level *negative* PV anomaly, as shown in Figs. 3 d, e, and f, and the associated upper-level *positive* geopotential anomaly, as shown in Figs. 4d, e, and f. These anomalies generally occur between the 150 and 200 hPa levels directly above the composite PV tower at each of the four times. These negative PV anomalies appear to develop following the passage, at upper levels around G-30h, of a positive PV anomaly (Fig. 3a). Thus, the composite cross-sections suggest that the development of an upper-level negative PV perturbation above the AEW PV tower portends disturbance intensification and perhaps the initiation of tropical cyclogenesis. The correlation between the intensification of lower and middle-tropospheric positive

PV and upper-level negative PV suggests that such an anomaly is likely generated by the AEW itself.

b) Steering flow

The steering flow of the wave composites at 6h, 18h, and 36h back from TD declaration were approximated using four different balanced layer-average techniques, similar to that used in CG: layer averages $((\mathbf{V}_{\text{top}} + \mathbf{V}_{\text{bot}}) / 2)$ for 500-700 hPa, 600-800 hPa, 500-1000 hPa, and 200-900 hPa. The results are displayed in Table 1.

CG demonstrated that a pressure-weighted layer average of 500-700 hPa winds at 5-7 degrees latitude radius from the center of a tropical cyclone provided the best correlation with the actual cyclone speed and direction. However, CG's results were based on a study of more mature tropical cyclones that are characterized by PV towers that extend throughout the depth of troposphere, leading to a reasonable assumption that the mid-tropospheric winds would give the best approximation. Examination of the four techniques shown in Fig. 5 supports CG's claim. The 500-700 hPa layer average winds provide the most accurate steering flow estimate at 6h back, when the wave composite PV tower extends close to the top of the troposphere, to about 250 hPa (Fig. 3d).

At G-18h, however, the PV tower extends vertically only to 300 hPa (Fig. 3c), and the 500-700 hPa estimate no longer provides an accurate prediction of the wave's direction of motion. In fact, none of the four layer average estimates provide an accurate direction estimate at 18h. At 36h back, the PV tower (ignoring the .2 contour that appears disorganized with respect to the rest of the tower) extends only to about 400 hPa. Therefore, as expected, a layer-average taken closer to the surface (600-800 hPa) provides a better correlation for both wave speed and direction. These results and those of CG, which employs pressure-weighted

² The presence of a vertical PV tower at G-00h may be due to the insertion of a bogus vortex upon TD declaration in to NCEP's final analysis. However, the pattern of development in the 2 hours to G-06h is consistent with a gradual strengthening of the TC.

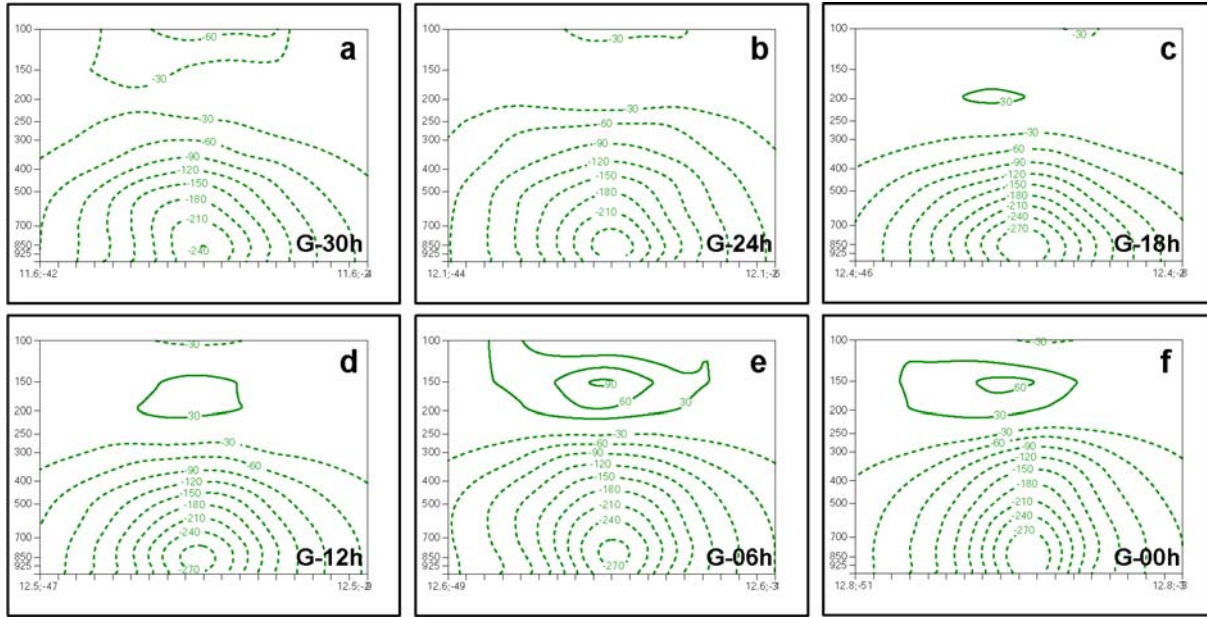


Figure 4. As in Fig. 3, except for perturbation geopotential height attributed to QGPV anomalies in Fig. 3 and boundary thermal perturbations (interval 30m, positive (negative) values solid (dashed)).

averaging rather than a pure layer-average for the first three techniques in Table 1, suggest that the most accurate steering flow approximation is obtained by averaging winds centered around the PV tower's mean pressure level. Finally, the 200-900 hPa average is inaccurate, as there is no reason to include 200 hPa winds in AEW steering flow estimates, as the PV tower does not extend that far into the atmosphere. CG performed a similar balanced average for this layer and obtained a high degree of inaccuracy in the steering flow estimate as well.

4. SUMMARY AND FUTURE WORK

Diagnosis of the PV structure of AEWs may provide insight into the mechanisms responsible for their development into TCs. It is hypothesized that the increase in AEW kinetic energy due to superposition of the AEW PV anomaly may be sufficient to initiate tropical cyclogenesis. As a first step toward investigating this hypothesis, a composite field of QGPV was created for 17 waves between 2000 and 2005 at 6-h intervals leading up to tropical depression declaration.

Analysis of the PV morphology and evolution indicates an progression towards a deeper, more upright and isotropic PV tower as the time of TD declaration nears. This evolution represents preliminary, qualitative evidence supporting the PV-compaction hypothesis. Furthermore, analysis of the upper-level anticyclonic PV anomaly that forms above the wave as it nears TD status may also provide clues into a particular wave's cyclogenetic potential.

In addition to including more AEWs into the composite, and evaluating the statistical significance of composite features, a future component of this work will sequester those AEW and mean-flow configurations that

promote development from those that do not. This examination of the evolution of non-developing waves may, in fact, reveal that the background flow serves to *inhibit* PV superposition, thus preventing the initiation of tropical cyclogenesis. Additionally, further investigation into the proper steering flow for these waves is needed to adequately determine what layers in the atmosphere play the most important role in the steering, and perhaps superposition, of AEW PV in their early stages of development.

Despite the qualitative success of the QGPV compositing and inversion to recover the steering flow, in order to make more realistic assessments of the role of the background flow and its interaction with AEW PV, a higher-order balance constraint is required. Future work will involve the construction of an Ertel PV composite of the AEWs that would be inverted under the constraint of non-linear balance that would be more appropriate for the tropics.

5. REFERENCES

Burpee, R. W., 1972: The origin and structure of easterly waves in the lower troposphere of North Africa. *J. Atmos. Sci.*, **29**, 77-90.

Layer Average Winds: $(V_{top} + V_{bot}) / 2$					
6 hours back	600/800 hPa	500/700 hPa	500/1000 hPa	200/900 hPa	<i>Actual</i>
Wind Speed (m/s)	7.37	7.87	5.93	4.8	8.58
Direction (deg N of W)	7.8	5.4	7.7	9.97	5.2
18 hours back					
Wind Speed (m/s)	8.53	8.95	5.65	6.02	8.86
Direction (deg N of W)	4.1	3.6	4.3	3.7	6.7
36 hours back					
Wind Speed (m/s)	8.88	9.46	5.95	6.06	8
Direction (deg N of W)	2.6	1.9	1.7	0	3.7

Table 1. Table of calculated steering flows taken at composite wave center at G-06h, G-18h, and G-36h back from TD declaration. Actual values of composite motion are in the right hand column, and values in bold represent best matches for a given time.

- Chan, J. C., and W. M. Gray, 1982: Tropical cyclone movement and surrounding flow relationships. *Mon. Wea. Rev.*, **110**, 1354-1374.
- Dole, R., 1993: Deformation in planetary scale flows. Preprints, *9th Conf. on Atmospheric and Oceanic Waves and Stability*, San Antonio, TX, Amer. Meteor. Soc., 1-4.
- Hakim, G., 2000: Climatology of coherent structures on the extratropical tropopause. *Mon. Wea. Rev.*, **128**, 385-406.
- Farrell, B., 1989: Transient development in confluent and diffluent flow. *J. Atmos. Sci.*, **46**, 3279-3288.
- Mak, M., and M. Cai, 1989: Local barotropic instability. *J. Atmos. Sci.*, **46**, 3289-3311.
- Reed, R. J., D. C. Norquist, and E. E. Recker, 1977: The structure and properties of African wave disturbances as observed during Phase III of GATE. *Mon. Wea. Rev.*, **105**, 317-333.
- Rennick, M. A., 1976: The generation of African waves. *J. Atmos. Sci.*, **33**, 1955-1969.
- Shapiro, L. J., 1977: Tropical storm formation from easterly waves: a criterion for development. *J. Atmos. Sci.*, **34**, 1007-1021.
- Sobel, A. H., and C. S. Bretherton, 1999: Development of synoptic-scale disturbances over the summertime Tropical Northwest Pacific. *J. Atmos. Sci.*, **56**, 3106-3127.
- Thorncroft, C. D., and B. J. Hoskins, 1994: An idealized study of African easterly waves: A linear view. *Quart. J. Roy. Meteor. Soc.*, **120**, 953-982.
- Wu, C., and K. A. Emanuel, 1995a: Potential vorticity diagnostics of hurricane movement. Part I: A Case study of Hurricane Bob (1991). *Mon. Wea. Rev.*, **123**, 69-92.
- Wu, C., and K. A. Emanuel, 1995b: Potential vorticity diagnostics of hurricane movement. Part II: Tropical Storm Ana (1991) and Hurricane Andrew (1992). *Mon. Wea. Rev.*, **123**, 93-109.

Acknowledgements

The authors thank Brett Hoover of the University of Wisconsin – Madison for his helpful discussions on comparisons of Ertel PV with QGPV during the course of this project. This work was supported by the National Science Foundation Grant ATM-0125169 and a 2005-2006 University of Wisconsin – Madison Undergraduate Hilldale Research Fellowship awarded to the first author.